

Article

# Phylogeography and Genetic Structure of the Swimming Crabs *Portunus sanguinolentus* (Herbst, 1783) in East Asia

Yu-Ming Lu <sup>1,†</sup>, Chun-Han Shih <sup>2,†</sup>, Po-Cheng Chen <sup>3,4,5,\*</sup>, Wei-Chieh Kao <sup>1</sup>, Ying-Chou Lee <sup>1</sup>, Yu-San Han <sup>1</sup>  
and Tzong-Der Tzeng <sup>6,†</sup>

<sup>1</sup> Institute of Fisheries Science, National Taiwan University, Taipei City 10617, Taiwan; d05b45003@ntu.edu.tw (Y.-M.L.); d09b45002@ntu.edu.tw (W.-C.K.); i812@ntu.edu.tw (Y.-C.L.); yshan@ntu.edu.tw (Y.-S.H.)

<sup>2</sup> Department of Leisure & Tourism Management, Shu-Te University, Kaohsiung 824, Taiwan; f92b45028@ntu.edu.tw

<sup>3</sup> Fisheries College, Jimei University, No. 185 Yinjiang Rd., Jimei District, Xiamen 361021, China

<sup>4</sup> Fujian Provincial Key Laboratory of Marine Fishery Resources and Eco-Environment, Xiamen 361021, China

<sup>5</sup> Third Institute of Oceanography, Ministry of Natural Resources, Xiamen 361005, China

<sup>6</sup> Department of Hospitality and Baking Management, Shu-Te University, Kaohsiung 824, Taiwan; tdtzeng@stu.edu.tw

\* Correspondence: d99241001@ntu.edu.tw

† These authors contributed equally to this work.

**Abstract:** The three-spot swimming crab (*Portunus sanguinolentus*) is mainly distributed in South East Asia. An analysis of mitochondrial control region partial sequences allows us to determine the population genetic structure, phylogeography and historical demography of this species in East Asia. The seven populations, which included 110 individuals, were collected from mainland China (Shanghai, SH, Xiamen, XM and Hong Kong, HK), Taiwan (Yilan, YL, Taichung, TC, Donggang, DG) and Singapore (Singapore, SGP). The nucleotide diversity ( $\pi$ ) of all individuals was 0.01149, with values ranging from 0.00372 (SGP) to 0.01345 (YL). In total, 90 haplotypes have been identified, which can be divided into two major lineages: lineage A consists of specimens from SH, YL, XM, TC and DG, and lineage B corresponds to specimen from SGP. From the second to the most recent interglacial period, population expansion was observed in each lineage. However, a low level of genetic differentiation was also observed in the three-spotted swimming crab, *P. sanguinolentus*, according to  $F_{ST}$  values. Our results suggest that several past and present habitat configurations have shaped the genetic patterns of *P. sanguinolentus* until now. During Pleistocene glaciations, when sea levels were low, this species may have moved along the coast from Southeast Asia to China. It first colonized the Hong Kong area during this era. After sea levels rose and shorelines receded, it subsequently spread to the coast of mainland China.

**Keywords:** *Portunus sanguinolentus*; historical demographic; population structure; population expansion



**Citation:** Lu, Y.-M.; Shih, C.-H.; Chen, P.-C.; Kao, W.-C.; Lee, Y.-C.; Han, Y.-S.; Tzeng, T.-D. Phylogeography and Genetic Structure of the Swimming Crabs *Portunus sanguinolentus* (Herbst, 1783) in East Asia. *J. Mar. Sci. Eng.* **2022**, *10*, 281. <https://doi.org/10.3390/jmse10020281>

Academic Editor: Paola Rumolo

Received: 20 January 2022

Accepted: 15 February 2022

Published: 18 February 2022

**Publisher's Note:** MDPI stays neutral with regard to jurisdictional claims in published maps and institutional affiliations.



**Copyright:** © 2022 by the authors. Licensee MDPI, Basel, Switzerland. This article is an open access article distributed under the terms and conditions of the Creative Commons Attribution (CC BY) license (<https://creativecommons.org/licenses/by/4.0/>).

## 1. Introduction

Complex geological events and climatic histories in different regions can help to shape the current phylogeographic patterns of marine organisms [1,2]. Therefore, climate change, biology and geography interact to affect the current genetic composition of a specific species [3]. Paleoclimate changes have contributed to the modern biodiversity patterns of the Asian continent and nearby islands [4]. Due to the fluctuation of sea levels in East Asia during the Pleistocene glacial era, the connection between the islands of Luzon, Hainan and Taiwan to the mainland has been repeatedly changed [5,6]. The Taiwan Strait was nearly separated from the Pacific Ocean, the South China Sea was completely exposed, and the main islands of Taiwan were connected to the mainland [7]. Complex geological and

climatic factors have led to ancient substitution and diffusion events, thus forming a highly diverse and unique biota [8]. These historical events seem to be the main reason for the genetic isolation, distribution and genetic structure of East Asian organisms [9].

During the Last Glacial Maximum (LGM), the sea level in the East China Sea was 130–150 m lower than its level at the present, and the sea level in the South China Sea was 100–120 m lower [10,11]. Therefore, the entire Yellow Sea, Bohai gulf, Tsushima and Taiwan Strait were exposed, and Japan, South Korea and Taiwan became connected to mainland China [12]. During the post-glacial period, coastal currents traveled from mainland China to the South China Sea, and the Chinese coastal stream flowed along Fujian to Vietnam. In addition, the thermohaline circulation in Singapore waters was important. Additionally, as many rivers were separated by the sea during the glacial period, but were connected during the interglacial period, gene flow may have been an inevitable result [13]. The determination of how past and current factors have contributed to observed genetic structures allows a deeper understanding of a species' evolutionary history and ecological adaptation, as well as the formulation of management and conservation strategies [14].

A species' genetic diversity is often shaped by past and current patterns of habitat availability and connectivity [2,3,7]. Extant patterns of population genetic diversity may be primarily shaped by historical processes, such as glaciations, climate changes and palaeogeographic formations [15–18]. Several recent studies suggested that climate change might cause significant changes in species distributions and biological richness, and DNA technology could also be used to track the genetic impact of adaptation [2,3]. Mitochondrial (mt) DNA has many characteristics, including rapid evolution, minimal recombination and maternal inheritance, making it suitable for population genetics research [19,20].

The three-spotted swimming crabs of the species *Portunus sanguinolentus*, which have been documented from East Africa to Hawaii, are widely distributed throughout the Indo-Pacific region [21–23]. *P. sanguinolentus* is one of the major crab species in China's East and South China Sea. This crab species is highly valuable in China, and its exports have increased since the 1990s. On the northern continental shelf of the South China Sea, crabs were analyzed for their composition and distribution in quantitative terms. *P. sanguinolentus* accounted for almost 30% of catches among all crab species [24]. After *P. trituberculatus*, *P. sanguinolentus* ranked high among the economically important crab species of the East China Sea in 1998 and 1999 [25]. However, fishing pressure has resulted in a decrease in the yield of *P. sanguinolentus* over the past few years [26].

Genetic diversity and its relationship to population genetic structure can be used to manage and protect a commercially important species [27,28]. Functional genetic diversity in an exploited marine species is relevant to fisheries management. Many studies on the reproductive biology [29], fisheries biology [30] and ecology [31] of *P. sanguinolentus* have been conducted. It is crucial to manage crab resources based on these data. By contrast, there is little information about the phylogeography and population genetic structure of *P. sanguinolentus* from Southeast Asia, East Asia and Northeast Asia. Using mtDNA fragments from the control region (D-loop) gene, we discovered the genetic structure of Southeast, East and Northeast Asia's three-spotted swimmer crab populations, along with their historical demography.

## 2. Materials and Methods

### 2.1. Sample Collection

Specimens were collected in public and open waters between December 2018 and October 2019 by utilizing five decoy pitfalls in each coastal and estuarine location from 17:00 to 7:30 successively, working three days a week. Seven populations that included 110 individuals from mainland China (Shanghai, SH, Xiamen, XM and Hong Kong, HK), Taiwan (Yilan, YL, Taichung, TC, Donggang, DG) and Singapore (Singapore, SGP) were collected (Figure 1; Table 1). DNA was extracted from the specimens after freezing or icing and kept at  $-75^{\circ}\text{C}$  immediately after capture.

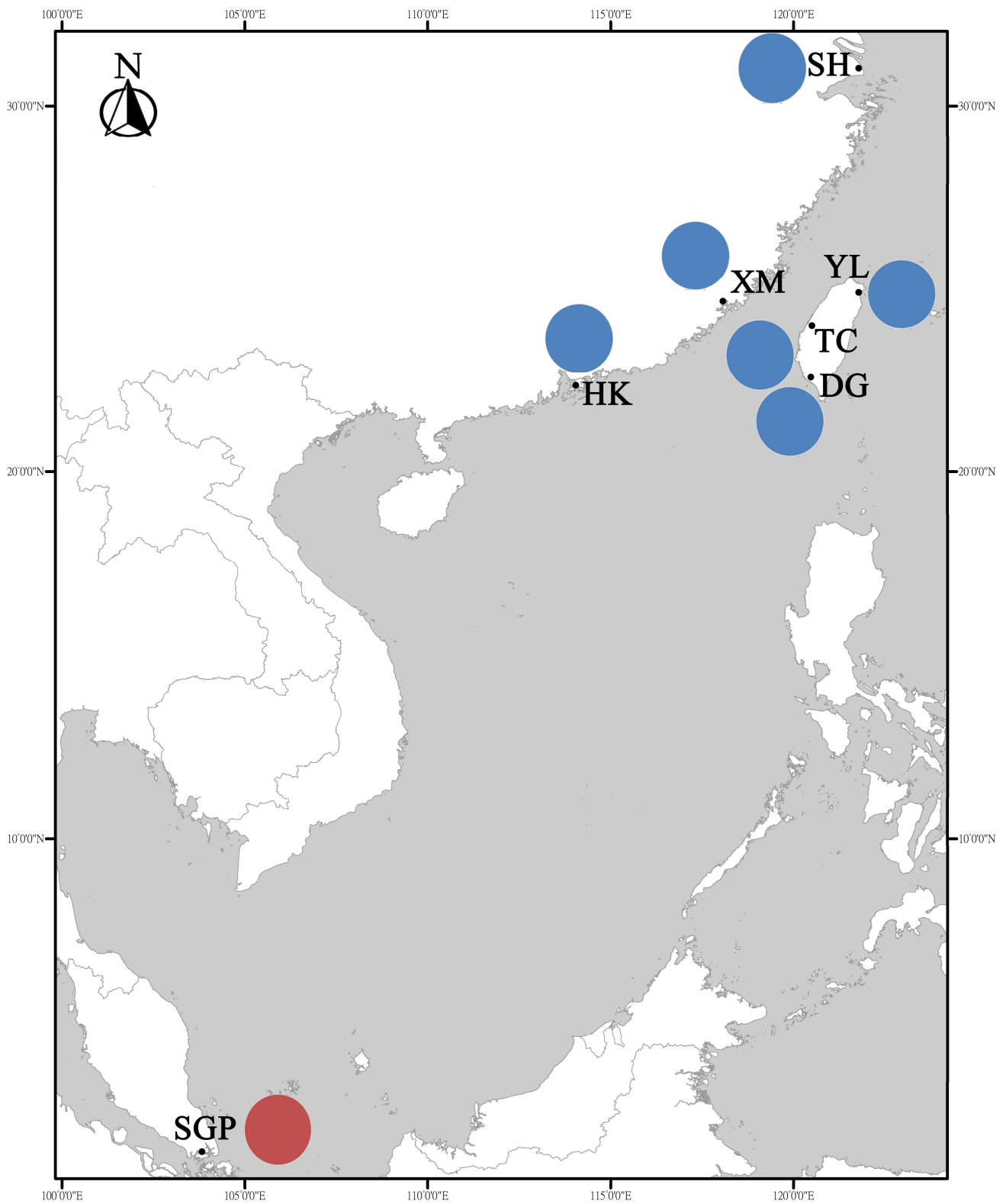


**Figure 1.** Sampling localities of *Portunus sanguinolentus* and haplotype frequencies in East Asia. In Table 1, the numbers of lineages A and B are also shown.

**Table 1.** Codes of sampling sites, sample sizes (*n*), number of haplotypes (*n<sub>h</sub>*), gene diversity (*h*), nucleotide diversity ( $\pi$ ) and Tajima’s *D* and Fu’s *F<sub>s</sub>* statistics for seven populations of *Portunus sanguinolentus* in East Asia.

Code	Sample Site	<i>n</i>	<i>n<sub>h</sub></i>	Lineage 1	Lineage 2	<i>h</i> Diversity	$\pi$ Diversity	Tajima’s <i>D</i>	Fu’s <i>F<sub>s</sub></i>
SH	Shanghai, China	18	14	18	0	0.961 ± 0.034	0.00478 ± 0.00097	−1.8221 *	−7.429 *
TC	Taichung, Taiwan	25	25	25	0	1.000 ± 0.011	0.00818 ± 0.00818	−1.6345	−22.885 **
XM	Xiamen, China	18	11	18	0	0.856 ± 0.079	0.00372 ± 0.00110	−1.7473	−4.134
DG	Donggang, Taiwan	16	13	16	0	0.967 ± 0.036	0.00596 ± 0.00088	−0.9149	−5.639 *
HK	Hong Kong, China	11	11	11	0	1.000 ± 0.039	0.00652 ± 0.00078	−0.7909	−6.454 *
YL	Yilan, Taiwan	15	15	15	0	1.000 ± 0.024	0.00909 ± 0.00111	−0.9552	−8.867 **
SGP	Singapore, Singapore	7	7	0	7	1.000 ± 0.076	0.01345 ± 0.00173	1.0533	−1.300
Lineage A		103	83			0.987 ± 0.006	0.00780 ± 0.00054	−2.1899 **	−114.956 **
Lineage B		7	7			1.000 ± 0.076	0.01345 ± 0.00173	1.0533	−1.300
Total		110	90			0.988 ± 0.005	0.01149 ± 0.00135	−2.04282 *	−105.649 **

\* *p* < 0.05, \*\* *p* < 0.01.

### 2.2. DNA Extraction, PCR and Sequencing

Using the QIAamp DNA Mini Kit, we extracted total genomic DNA from the pereopod muscle [32]. The mitochondrial DNA were amplified and sequenced. The control region fragments of mtDNA were then amplified and sequenced. The control region sequence was amplified using YEN-F (5'- GCA AAT ACA CGC AAT AAC TCT CAT AC -3') and YEN-B (5'- TGT AAA TCC GTT ACG AAT AAT ATA GG -3') primers. Thermal loop measurements were carried out using a Geneamp 2400 thermal loop device (Perkin Elmer, Norwalk, CT, USA). In the PCR reaction, a total of 39 denatured rings were run at 95 °C for 50 s, the annealing step was completed at 50 °C for 1 min, and the extension was completed at 72 °C for 1.5 min. The first and last loops included an initial denaturation step of 5 min at 95 °C and a final extension of 10 min at 72 °C, respectively. By separating PCR products on 1.5% agarose gel electrophoresis, purifying them with a gene clean II kit (Bio101), and sequencing them with an ABI 377 DNA sequencer, we were able to identify mRNAs identified in the PCR products.

### 2.3. Analyses of Sequences

Megalign (DNASTAR, LaserGene, WI, USA) was used to align all sequences. The number, base composition, haplotype and nucleotide diversity [33] of variable and parsimony information sites were identified using calculations that were performed with DnaSP version 5.00 [34]. Some sequences of the control region genes were concatenated in the following analysis. Using MEGA 6, the neighbor-joining (NJ) and maximum likelihood (ML) methods were applied to analyze the geographic characteristics of the control area [35,36]. The phylogenetic relationships of all haplotypes were assessed using bootstrap analysis of 1000 replicates. Using the optimal substitution model determined using MEGA, networks were constructed using the median-joining method in Fluxus-Engineering networks version 4.6.1.3. In the ARLEQUIN program, the frequency distribution of pairwise differences (mismatch distribution) between sequences was examined for historical demographic expansion [7,37]. We used the formula  $A = \mu\pi$  [38] to estimate the approximate age of the population or lineage, where *A* represents the age of the population or lineage,  $\pi$  represents the nucleotide diversity and  $\mu$  is  $\mu$  (mutation rate) × generation time; formula  $\tau = 2\mu T$  [39] estimates the approximate date of population expansion, where *T* represents the time since the expansion,  $\tau$  is the extension time, and  $2\mu$  is  $\mu$  (the mutation rate) × generation time × the number of bases sequenced. The mutation rate of the nucleotide of the D-loop is 3.6% per myr, which is the average mutation rate of fish [40]. In the analysis of divergence rates, a mean mutation rate of 3.6% per myr was applied to the divergence rates of all of the D-loop sequences, and a generation time of one year was assumed [41,42]. The ARLEQUIN software version 3.5 was used to estimate pair-wise *F<sub>ST</sub>* statistics in order to assess the genetic differentiation between two populations [43]. We assessed the structure of the population by molecular analysis of variance (AMOVA in ARLEQUIN; [44]) as well as by

constructing a dendrogram for each point in our sample using an unweighted arithmetic mean based on  $F_{ST}$  values (UPGMA).

UPGMA trees for these seven populations provide information about their groupings. Hypothetical display groups with  $\Phi_C$  maxima that are significantly different from random tissues from similar populations are most likely to represent geographical subdivisions [45]. The permutation test was used for evaluation, and the significance test of the results, was evaluated via 10,000 random permutation tests. By testing for deviations from neutrality, Tajima's  $D$  [46] can indicate if a population expansion had previously occurred. We also used Fu's  $F_s$  test [47] to evaluate the evidence for population expansion by DnaSP. In order to determine whether the population is expanding, DnaSP was used; as a measure of deviation from neutrality, we used Tajima's  $D$  test [46], which indicates whether population expansions occurred previously. Fu's  $F_s$  test [47] was used to determine whether DnaSP evidence indicated population expansion. Additionally, using DnaSP, we examined, by way of mismatch analysis, the frequency distribution of the nucleotide differences with respect to frequency. Geographic distances were paired 1000 times to determine significance levels, and the significance level was determined using the pairwise  $F_{ST}$  value and paired geographic distance values. The Mantel test [48] was used to test distance isolation. The approximate geographical distance between sampling sites was used as the minimum distance map.

### 3. Results and Discussions

#### *Biological Information and Growth Estimation*

We sequenced 110 specimens and obtained the following results. For the control region of 864 bp, we found 57 variable sites and 71 parsimony informative sites, totaling 90 distinct haplotypes (S1 Dataset). GeneBank accession numbers OL692628–OL692737 contain all of the sequences deposited. Among the seven populations evaluated, the nucleotide compositions had an AT bias (with G + C content of 33.7%). The haplotypic diversity ( $h$ ) of all seven populations was 0.988, with values ranging from 0.856 (XM) to 1.000 (YL, TC, HK and SGP) (Table 1).

A nucleotide diversity of 0.011 was found across all populations ( $\pi$ ), with values ranging from 0.004 (XM) to 0.013 (SGP) (Table 1). A total of 90 haplotypes was detected in 110 samples. The most common genotype was shared by 11 individuals across 3 populations, including XM (7), SH (3) and SGP (3).

We used the T92 model to explain the best-fitting modes of our data. The model was used for both NJ and ML rebuilding as well as for the AMOVA study. Both NJ and ML trees had very similar results (Figure 2). Two distinct lineages were identified (A and B). Based on the NJ and ML trees, the bootstrap values were 99 and 100, respectively, for lineages A and B. The network of all specimens (Figure 3) confirms the findings of these phylogenetic trees. In lineage A, two sub-lineages were found. Figure 1 and Table 1 show the distribution of specimens of lineages A and B for different populations. Lineage A included all the individuals from SH, YL, TC, XM, DG and HK, and all the individuals from SGP were only involved in lineage B.

Accordingly, lineages A and B had haplotype diversities ( $h$ ) of 0.987 and 1.000, respectively, and the nucleotide diversity ( $\pi$ ) of each was respectively 0.008 and 0.013 (Table 1). The  $\tau$  values of lineages A and B were 4.035/2 and 8.136/2 generations, respectively (Table 1). The  $\tau$  values of lineages A and B were 4.035/2 $\mu$  and 8.136/2 $\mu$  generations, respectively, using an average mutation rate of 3.6%/myr and a generation time of 1 year. For lineage A, the time of expansion was approximately 160,022 years ago, and for lineage B, it was approximately 322,744 years ago. The  $F_{ST}$  values within the seven populations were all significant (Table 2). In terms of the UPGMA tree of these seven sampling areas, two major groups were identified (Figure 4); the first group includes XM, TC, SH, DG, HK and YL, and the second group includes SG.

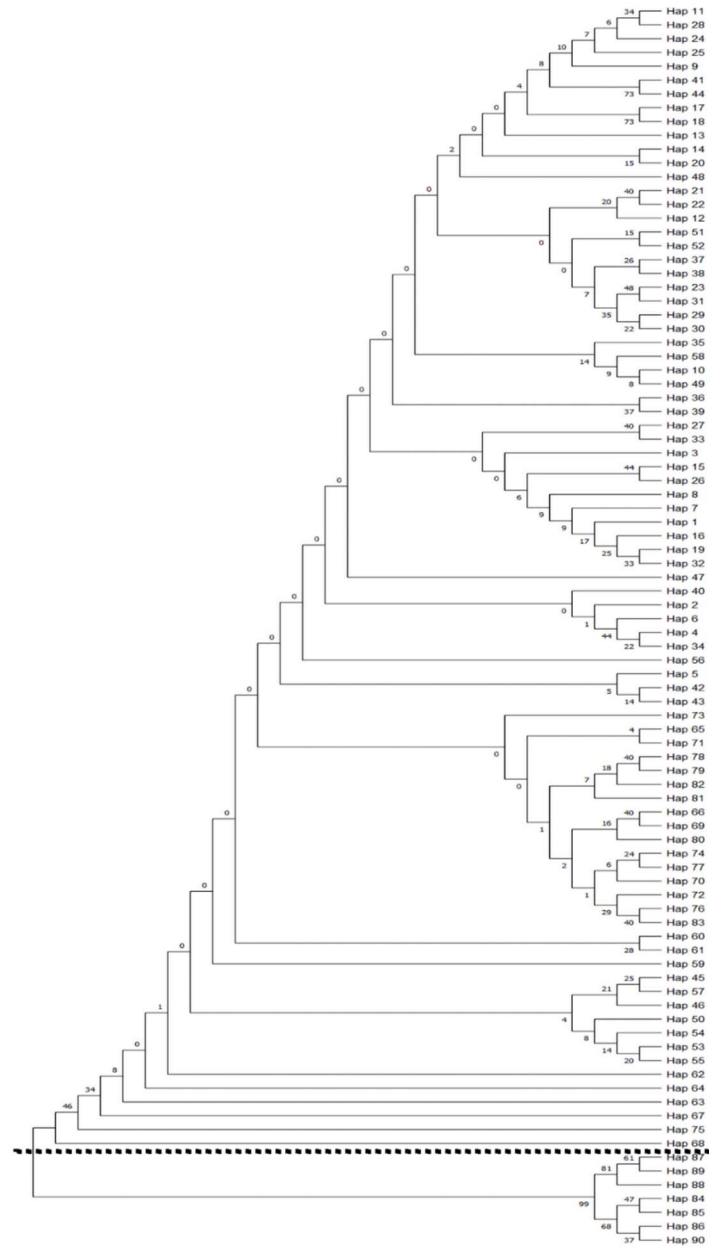


**Figure 2.** Neighbor-joining (NJ) tree based on control region gene sequences with bootstrap values (NJ/ML, respectively) for *P. sanguinolentus*.

**Table 2.** The matrices shown below show pairwise  $F_{ST}$  (below diagonal) and  $p$  values (above diagonal) for seven populations of *P. sanguinolentus* in East Asia.

	SH	YL	XM	TC	DG	HK	SGP
SH	-	0.000	0.000	0.000	0.000	0.000	0.000
YL	0.354	-	0.000	0.000	0.000	0.000	0.000
XM	0.063	0.342	-	0.036	0.000	0.000	0.000
TC	0.055	0.242	0.030	-	0.000	0.000	0.000
DG	0.182	0.274	0.136	0.075	-	0.000	0.000
HK	0.321	0.153	0.315	0.198	0.167	-	0.000
SGP	0.790	0.734	0.822	0.742	0.767	0.739	-

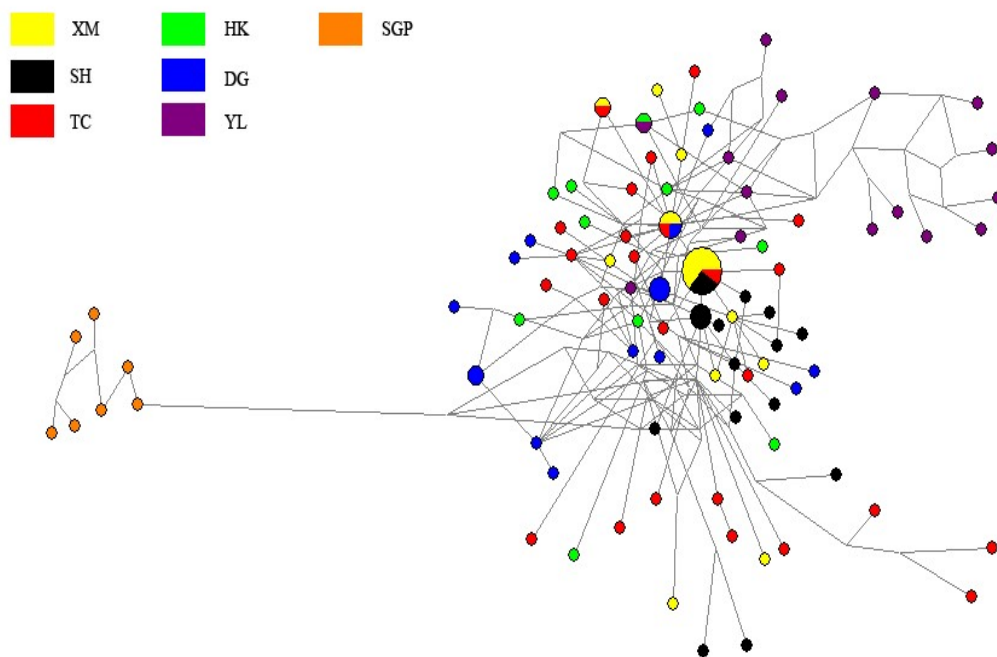


**Figure 3.** The haplotype network of *Portunus sanguinolentus* in all sampling sites.

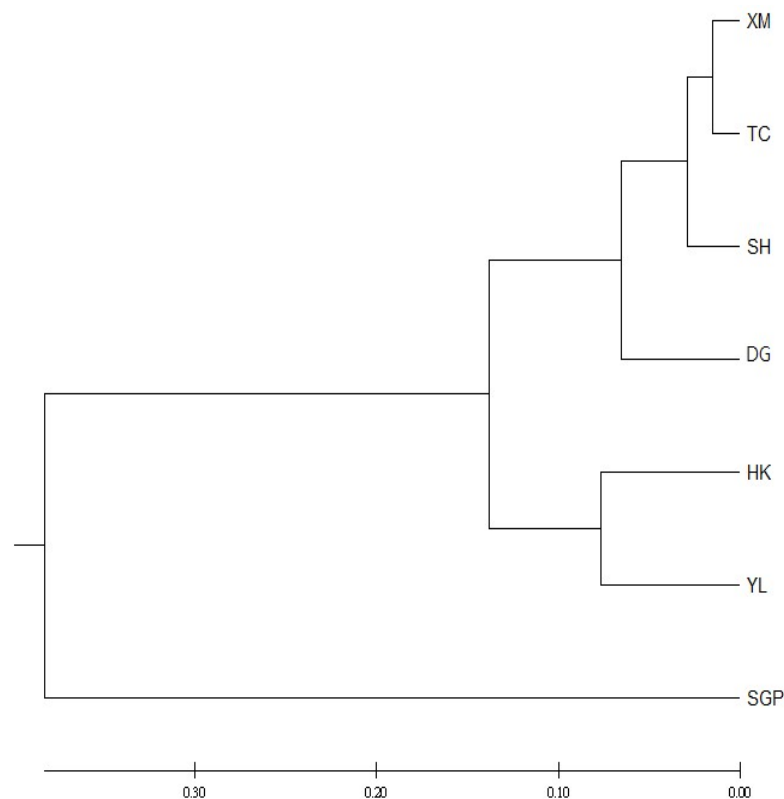


**Figure 4.** The relationships between seven sampling sites are shown in an UPGMA tree.

It is possible to further divide the first group into two subgroups. One of the subgroups of the first group included the XM, TC, SH and DG populations; the second subgroup included the HK and YL populations. According to the UPGMA trees, five different groupings could be detected among the seven populations listed in Table 3. Based on the AMOVA analysis, the  $F_{ST}$  for seven pair-wise population was 0.4259, indicating significant heterogeneity in at least one case. Significant values of  $\Phi_{CT}$  were observed in all groupings.

**Table 3.** The results of AMOVA for *P. sanguinolentus* in seven populations in East Asia.

Population	Grouping	Source of Variation	Percentage of Variation	$\Phi$ -Statistics	$p$ (More-Extreme Value)
One group	Group 1{SH, YL, TC, XM, DG, HK, SGP}	AP	42.59	$\Phi_{ST} = 0.42592$	***
		WP	57.41		
Two groups	Group 1{SH, YL, TC, XM, DG, HK} Group 2 {SGP}	AG	75.19	$\Phi_{CT} = 0.75194$	***
		AP/WG	4.45	$\Phi_{SC} = 0.17932$	***
		WP	20.36	$\Phi_{ST} = 0.79643$	***
Three groups	Group 1 {SH, XM, TC, DG} Group 2 {HK, YL} Group 3 {SGP}	AG	52.28	$\Phi_{CT} = 0.52277$	***
		AP/WG	4.27	$\Phi_{SC} = 0.08937$	***
		WP	43.46	$\Phi_{ST} = 0.56542$	***
		AG	45.71	$\Phi_{CT} = 0.45707$	***
Four groups	Group 1{SH, XM, TC} Group 2 {DG} Group 3{HK, YL}	AP/WG	4.05	$\Phi_{SC} = 0.07457$	***
		WP	50.24	$\Phi_{ST} = 0.49755$	***
		AG	40.23	$\Phi_{CT} = 0.40227$	***
Five groups	Group 1{SH} Group 2 {XM, TC} Group 3{DG} Group 4{HK, YL} Group 5{SGP}	AP/WG	5.16	$\Phi_{SC} = 0.08627$	***
		WP	54.62	$\Phi_{ST} = 0.45384$	***
		AG	40.23	$\Phi_{CT} = 0.40227$	***
		AP/WG	5.16	$\Phi_{SC} = 0.08627$	***
		WP	54.62	$\Phi_{ST} = 0.45384$	***

AG is the among-group component of variance; AP/WG is the among-populations/within-group component of variance; and WP is the within-population component of variance. \*\*\*  $p < 0.001$  by the permutation test.

Based on the AMOVA analysis, the  $F_{ST}$  for each pair-wise population was 0.4259, indicating that there was significant heterogeneity in at least one paired population. All  $\Phi_{CT}$  values were observed to reach significance. According to the study, grouping 2 had the highest  $\Phi_{CT}$  (0.7519), and two groups could properly be divided into the following populations: the first group included SH, YL, TC, XM, DG and HK, whereas the second group included the SGP one. There were also significant  $\Phi_{CT}$  values among different groups, indicating that it may also have happened among populations that there was an additional genetic discontinuity. Table 1 shows that values of Tajima’s  $D$  were non-significant, except for SH (Table 1). Tajima’s  $D$  values were significant across each lineage and across the entire sample. Fu’s  $F_s$  tests were significant for the SH, TC, DG, HK and YL populations. The bimodal distribution of mismatched specimens was obtained for all specimens (Figure 5), with one mode representing differences between lineages and another mode representing differences within lineages. For lineage A or B, a unimodal distribution was obtained.

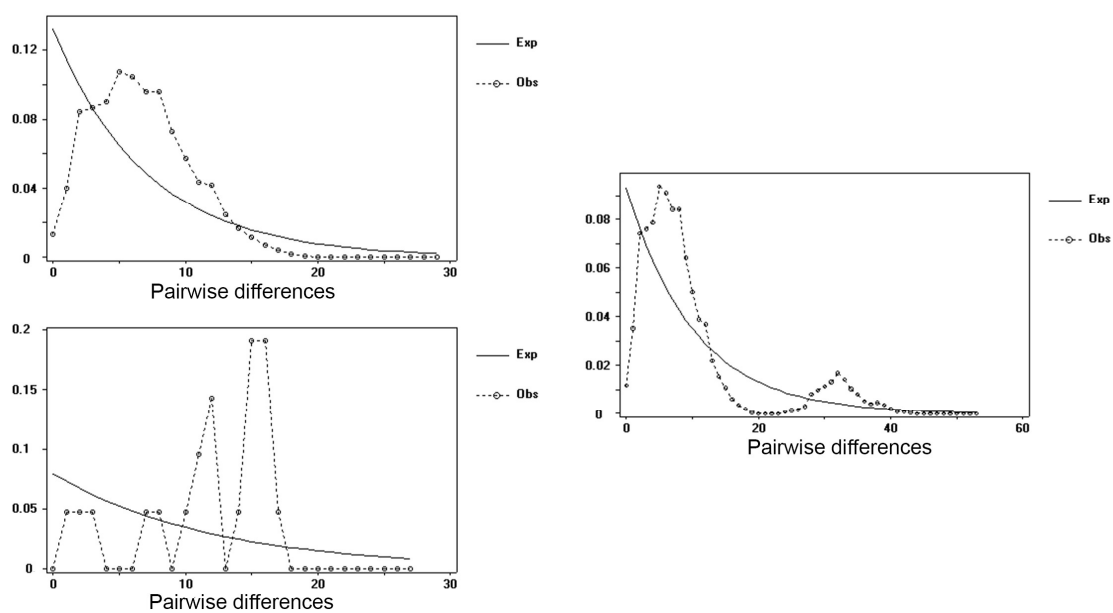


**Figure 5.** A sudden expansion model of the swimming crab *P. sanguinolentus* predicts the observed pair-wise differences and mismatch distributions.

#### 4. Discussions

The present study found two distinct lineages of *P. sanguinolentus* in East Asia (A and B), which agrees with the previous study [49]. Despite the fact that all seven populations did include individuals from lineages A and B, two distinct lineages (Figures 1–3) were detected. The SH, YL, TC, XM, DG and HK populations were only found to belong to lineage A, and the SGP population was only represented by individuals from lineage B.

All the populations of lineage A (the XM, SH and TC populations) shared the same most common allele, indicating that they were ancestrally related. There is evidence that populations containing ancestral genotypes tend to retain a higher level of haplotype and nucleotide diversity over time [50–52]. Compared to lineage A ( $\pi = 0.008$ ), nucleotide diversity ( $\pi = 0.013$ ;  $h = 1.000$ ) in lineage B was significantly higher than haplotype diversity ( $h = 0.987$ ). This indicates that lineage B is older than lineage A. Estimates are 160,022 and 322,744 years for the extension of lineages A and B, respectively.

The matching distribution of two different lineages indicates that a smaller population existed before the bottleneck or expansion of lineage A (Figure 5) [39]. According to this image, lineage A may have undergone expansion more recently than lineage B. This is also corroborated by the fact that the pairwise distribution pattern shifts toward being displaced to the right in Figure 5. Based on these findings, lineage A expanded for a longer period than lineage B. In other words, lineage B only experienced gene flow exchanges but did not experience population expansion. Since there are few samples, it is likely that there are multiple peaks in pair-wise differences and the expected distribution of mismatches for lineage B.

The currents in the planktonic larval stage of *P. sanguinolentus* in the study area include the offshore warm current of China and the South China Sea warm current. Therefore, offshore plankton larvae may be transported along the ocean currents, which bring low salinity to the south along the coast of China [53,54]. Genetic exchange in the marine environment may be due to the high transmission capacity of *P. sanguinolentus* larvae and the lack of physical barriers. The lack of genetic structure in marine ecosystems is usually due to limitations of physical barriers, larvae dispersal abilities and their ability to swim long distances [55]. Similar results have often appeared in previous studies; for example, the red crab *Charybdis feriata* found on the coast of the China Sea also demonstrated the phenomenon of low genetic differentiation [56]. The evolutionary age of lineage B is much older than lineage A (approximately 160,022 and 322,744 years ago, respectively), because during the Last Glacial Maxima, the continents of China and SE Asia were an exposed landmass [57]. After sea levels rose, these coastlines were immersed by the sea again, and lineage A developed in Northeast Asia and Southeast Asia. Probably after lineage A developed, it dispersed via the South China Sea warm currents and China coastal current to HK, XM, DG, TC and SH waters. Therefore, the oldest and youngest populations were those from SPG and XM, respectively.

Furthermore, the distribution limit of lineage B probably could not extend to the Indian Ocean through the Malacca Strait. During the glacial maxima, the sunda shelf was blocked [58]. After the sea level rose, lineage B could invade the new coastlines but their larvae could not travel through the Malacca Strait to the Indian Ocean. A similar pattern was also revealed for the tiger prawn, where there was a sharp genetic break at the west coast of the Malacca Strait [58]. Then, lineage B was probably only distributed in the South China Sea, and did not extend to the West Pacific (lineage A). Marine species were restricted into relatively confined areas as a result of habitat destruction, which resulted in the mixing of populations and reduced genetic variation [59]. After LGM, the distribution of three-spot swimming crabs gradually extended, corresponding to the rise of the sea level of the East China Sea. The swimming crab migrates from the inshore to the offshore as it reaches a certain size or life stage, but the distance is limited [60]. In this species, therefore, gene flow occurs primarily through larval dispersal. Ocean currents play a key role in dispersal. The life span of *P. sanguinolentus* is about 1–2 years. It usually inhabits sandy marine habitats at depths of 10–80 m [61–63]. The larvae drift with the ocean current.

After 15–18 days, the hatched zoeae transform into giant crabs called juvenile crabs, which gradually transition to living on the bottom of the sea [29]. Therefore, the planktonic larval stage of crabs may have an impact on determining the genetic structure. Coastal currents shifted from mainland China to the South China Sea during the post-glacial period. The Chinese coastal stream flows along Fujian to Vietnam. The role of thermohaline circulation in the waters of Singapore is an important function. However, the interaction between the DG sample in Taiwan and the coastal current in China was not obvious in lineage A, resulting in the formation of the isolated group of lineage B.

Based on the above discussions, the expansion path of lineage A was carried by the Kuroshio Current from the southern end to Taiwan and then divided into three tributaries: one flowed through the east of Taiwan, one flowed to the west, forming the HK and YL populations that are relatively similar, and the last one flowed up the Taiwan Strait and the coastal waters of China to SH. For Lineage B, this means that SGP did not expand, but only formed a gene flow interaction. However, other marine organisms demonstrated similar patterns with two main lineages. As examples, barnacles [64,65] and intertidal crabs [66] have different lineages in the East, Northeast and Southeast Asia Sea and their populations in East and Northeast Asia are much younger. It is phylogeography important for the management and conservation of the commercial species of *P. sanguinolentus* along Asian coasts to determine where it originated from and its genetic structure.

## 5. Conclusions

Based on our study, we found two major lineages (A and B) among the three spot crab populations in East Asia. Lineage B is generally older than lineage A. The A and B lineages of the three-spotted swimming crab *P. sanguinolentus* underwent population expansion approximately during the Pleistocene glacial period (approximately 160,022 and 322,744 years ago, respectively). The genetic structure of *P. sanguinolentus* in East Asia may have been affected during the Pleistocene Glacial Maxima and due to ocean currents that blocked larval dispersal pathways, resulting in the evolution of lineage B into a single population, with marine species confined to relatively narrow areas, resulting in mixed populations with reduced genetic variation.

**Author Contributions:** Conceptualization, Y.-M.L., C.-H.S., P.-C.C. and T.-D.T.; methodology, Y.-M.L., C.-H.S., P.-C.C. and T.-D.T.; software, Y.-M.L., C.-H.S. and P.-C.C.; validation, Y.-M.L., C.-H.S., P.-C.C., W.-C.K., Y.-C.L. and T.-D.T.; formal analysis, Y.-M.L., C.-H.S., P.-C.C., W.-C.K., Y.-C.L. and T.-D.T.; investigation, Y.-M.L., C.-H.S., P.-C.C., W.-C.K., Y.-C.L. and T.-D.T.; resources, Y.-M.L., C.-H.S. and P.-C.C.; data curation, Y.-M.L., C.-H.S. and P.-C.C.; writing—original draft preparation, Y.-M.L., C.-H.S. and P.-C.C.; writing—review and editing, Y.-M.L., C.-H.S., Y.-S.H. and P.-C.C.; visualization, Y.-M.L., C.-H.S. and P.-C.C.; supervision, Y.-M.L., C.-H.S., P.-C.C. and T.-D.T.; project administration, Y.-M.L., C.-H.S., P.-C.C. and T.-D.T.; funding acquisition, Y.-M.L., C.-H.S., P.-C.C. and T.-D.T. All authors have read and agreed to the published version of the manuscript.

**Funding:** This work was supported by the Ministry of Science and Technology, grant number MOST 110-2121-M-366-001. The funders had no role in study design, data collection and analysis, decision to publish, or preparation of the manuscript.

**Institutional Review Board Statement:** Not applicable.

**Informed Consent Statement:** Not applicable.

**Data Availability Statement:** Not applicable.

**Acknowledgments:** We thank the Global Institute for Green Tourism, University of California, Berkeley, for supporting the cruises of the biological survey. We would also like to thank the anonymous reviewers, whose useful suggestions were incorporated into the manuscript.

**Conflicts of Interest:** The authors declare no conflict of interest.

## References

1. Hewitt, G.M. Some genetic consequences of ice ages, and their role in divergence and speciation. *Biol. J. Linn. Soc.* **1996**, *58*, 247–276. [[CrossRef](#)]
2. Avise, J.C. *Phylogeography: The History and Formation of Species*, 3rd ed.; Harvard Publishers Inc.: Cambridge, MA, USA, 2000.
3. Hewitt, G.M. The genetic legacy of the quaternary ice ages. *Nature* **2000**, *405*, 907–913. [[CrossRef](#)] [[PubMed](#)]
4. Gallagher, S.J.; Kitamura, A.; Iryu, Y.; Itaki, T.; Koizumi, I.; Hoiles, P.W. The Pliocene to recent history of the Kuroshio and Tsushima Currents: A multi-proxy approach. *Prog. Earth Planet. Sci.* **2015**, *2*, 2–17. [[CrossRef](#)]
5. Hansen, J.E.; Sato, M. 2012 Paleoclimate Implications for human-made climate change. In *Climate Change: Inferences from Paleoclimate and Regional Aspects*; Berger, A., Mesinger, F., Sijacki, D., Eds.; Springer Publishers Inc.: Berlin/Heidelberg, Germany, 2012.
6. Wang, L.; Sarnthein, M.; Erlenkeuser, H.; Grimalt, J.; Grootes, P.; Heilig, S.; Ivanova, E.; Kienast, M.; Pelejero, C.; Pflaumann, U. East Asian monsoon climate during the late Pleistocene: High-resolution sediment records from the South China Sea. *Mar. Geol.* **1999**, *156*, 245–284. [[CrossRef](#)]
7. Chen, P.C.; Shih, C.H.; Chu, T.J.; Wang, D.; Lee, Y.C.; Tzeng, T.D. Population Structure and Historical Demography of the Oriental River Prawn (*Macrobrachium nipponense*) in Taiwan. *PLoS ONE* **2015**, *10*, e0145927. [[CrossRef](#)]
8. Li, Y.; Chen, J.; Jiang, L.; Qiao, G. Islands conserve high species richness and areas of endemism of *Hormaphidinae* aphids. *Curr. Zool.* **2017**, *63*, 623–632. [[CrossRef](#)]
9. Shen, K.N.; Jamandre, B.W.; Hsu, C.C.; Tzeng, W.N.; Durand, J.D. Plio-Pleistocene sea level and temperature fluctuations in the northwestern Pacific promoted speciation in the globally-distributed fathead mullet *Mugil cephalus*. *BMC Evol. Biol.* **2011**, *11*, 83. [[CrossRef](#)]
10. Xiao, S.; Li, A.; Jiang, F.; Li, T.; Wan, S.; Huang, P. The history of the Yangtze river entering sea since the last glacial maximum: A review and look forward. *J. Coast. Res.* **2004**, *20*, 599–604. [[CrossRef](#)]
11. Liu, M.Y.; Cai, Y.; Tzeng, C.S. Molecular systematics of the freshwater prawn genus *Macrobrachium* Bate, 1868 (Crustacea: Decapoda: Palaemonidae) inferred from mtDNA sequences, with emphasis on east Asian species. *Zool. Stud.* **2007**, *46*, 272–289.
12. Wang, P.; Sun, X. Last glacial maximum in China: Comparison between land and sea. *Catena* **1994**, *23*, 341–353.
13. Craw, D.; Burrige, C.; Anderson, L.; Waters, J.M. Late Quaternary river drainage and fish evolution, Southland, New Zealand. *Geomorphology* **2007**, *84*, 98–110. [[CrossRef](#)]
14. McCartney-Melstad, E.; Shaffer, B.H. Amphibian molecular ecology and how it has informed conservation. *Mol. Ecol.* **2015**, *24*, 5084–5109. [[CrossRef](#)] [[PubMed](#)]
15. Strugnell, J.M.; Watts, P.C.; Smith, P.J.; Allcock, A.L. Persistent genetic signatures of historic climatic events in an Antarctic octopus. *Mol. Ecol.* **2012**, *21*, 2775–2787. [[CrossRef](#)] [[PubMed](#)]
16. Pincheel, T.; Vanschoenwinkel, B.; Waterkeyn, A.; Vanhove, M.P.M.; Pinder, A.M.; Timms, B.V. Fairy shrimps in distress: A molecular taxonomic review of the diverse fairy shrimp genus *Branchinella* (Anostraca: *Thamnocephalidae*) in Australia in the light of ongoing environmental change. *Hydrobiologia* **2013**, *700*, 313–327. [[CrossRef](#)]
17. Pineros, V.J.; Gutierrez-Rodriguez, C. Population genetic structure and connectivity in the widespread coral-reef fish *Abudefduf saxatilis*: The role of historic and contemporary factors. *Coral Reefs* **2017**, *36*, 877–890. [[CrossRef](#)]
18. Nali, R.C.; Becker, C.G.; Zamudio, K.R.; Prado, C.P.A. Topography, more than land cover, explains genetic diversity in a Neotropical savanna tree frog. *Divers. Distrib.* **2020**, *26*, 1798–1812. [[CrossRef](#)]
19. Hoelzel, A.R.; Hancock, J.M.; Dover, G.A. Evolution of the cetacean mitochondrial D-loop region. *Mol. Biol. Evol.* **1991**, *8*, 475–493.
20. Xu, J.; Chan, T.Y.; Tsang, L.M.; Chu, K.H. Phylogeography of the mitten crab *Eriocheir sensu stricto* in East Asia: Pleistocene isolation, population expansion and secondary contact. *Mol. Phylogenet. Evol.* **2009**, *52*, 45–56. [[CrossRef](#)]
21. Apel, M.; Spiridonov, V.A. Taxonomy and zoogeography of the portunid crabs (Crustacea: Decapoda: *Brachyura: Portunidae*) of the Arabian Gulf and the adjacent waters. *Fauna Arabia* **1998**, *17*, 159–331.
22. Lai, J.C.Y.; Ng, P.K.L.; Davie, P.J.F. A revision of the *Portunus pelagicus* (Linnaeus, 1758) species complex (Crustacea: Brachyura: Portunidae), with the recognition of four species. *Raffles Bull. Zool.* **2010**, *58*, 199–237.
23. Huang, Y.H.; Shih, H.T. Diversity in the Taiwanese swimming crabs (Crustacea: *Brachyura: Portunidae*) estimated through DNA barcodes, with descriptions of 14 new records. *Zool. Stud.* **2021**, *60*, 60.
24. Huang, Z.R. Species composition and quantitative distribution of crabs in the northern continental shelf of South China Sea. *J. Dalian Fish Univ.* **2009**, *24*, 553–558.
25. Yu, C.G.; Song, H.T.; Yao, G.Z.; Lü, H.Q. Composition and distribution of economic crab species in the East China Sea. *Oceanol. Limnol. Sin.* **2006**, *37*, 53–60.
26. Yang, C.P.; Li, H.X.; Li, L.; Xu, J.; Yan, Y. Population structure, morphometric analysis and reproductive biology of *Portunus sanguinolentus* (Herbst, 1783) (Decapoda: Brachyura: Portunidae) in Honghai Bay, South China Sea. *J. Crustacean Biol.* **2014**, *34*, 722–730. [[CrossRef](#)]
27. Ward, R.D. Genetics in fisheries management. *Hydrobiologia* **2000**, *420*, 191–201. [[CrossRef](#)]
28. Ortega-Villaizan Romo, M.; Suzuki, S.; Nakajima, M.; Taniguchi, N. Genetic evolution of inter individual relatedness for broodstock management of the rare species barfin flounder *Verasper moseri* using microsatellite DNA markers. *Fish. Sci.* **2006**, *72*, 33–39. [[CrossRef](#)]

29. Rasheed, S.; Mustaquim, J. Size at sexual maturity, breeding season and fecundity of three-spot swimming crab *Portunus sanguinolentus* (Herbst, 1783) (Decapoda, Brachyura, Portunidae) occurring in the coastal waters of Karachi, Pakistan. *Fish Res.* **2010**, *103*, 56–62. [[CrossRef](#)]
30. Lee, H.H.; Hsu, C.C. Population biology of the swimming crab *Portunus sanguinolentus* in the waters off northern Taiwan. *J. Crustaceana Biol.* **2003**, *23*, 691–699. [[CrossRef](#)]
31. Song, H.T.; Yu, C.G.; Xue, L.J.; Yao, G.Z. *The Economical Shrimp and Crab from East China Sea*; Ocean Press: Beijing, China, 2006.
32. Sambrook, J.; Russell, D.W. *Molecular Cloning: A Laboratory Manual*, 3rd ed.; Cold Spring Harbor Publishers Inc.: New York, NY, USA, 2001.
33. Nei, M. *Molecular Evolutionary Genetics*, 1st ed.; Columbia Publishers Inc.: New York, NY, USA, 1987.
34. Rozas, J.; Sanchez-Delbarrio, J.C.; Messeguer, X.; Rozas, R. DnaSP, DNA polymorphism analyses by the coalescent and other methods. *Bioinformatics* **2003**, *19*, 2496–2497. [[CrossRef](#)]
35. Tamura, K.; Peterson, D.; Peterson, N.; Stecher, G.; Nei, M.; Kumar, S. MEGA6: Molecular evolutionary genetics analysis using maximum likelihood, evolutionary distance, and maximum parsimony methods. *Mol. Biol. Evol.* **2011**, *28*, 2731–2739. [[CrossRef](#)]
36. Bandelt, H.J.; Forster, P.; Rohlf, A. Median-joining networks for inferring intraspecific phylogenies. *Mol. Biol. Evol.* **1999**, *16*, 37–48. [[CrossRef](#)] [[PubMed](#)]
37. Chen, P.C.; Shih, C.H.; Chu, T.J.; Lee, Y.C.; Tzeng, T.D. Phylogeography and genetic structure of the oriental river prawn *Macrobrachium nipponense* (Crustacea: Decapoda: Palaemonidae) in East Asia. *PLoS ONE* **2017**, *2*, e0173490. [[CrossRef](#)] [[PubMed](#)]
38. Nei, M.; Tajima, F. DNA polymorphism detectable by restriction endonucleases. *Genetics* **1981**, *97*, 145–163. [[CrossRef](#)] [[PubMed](#)]
39. Rogers, A.R.; Harpending, H. Population growth makes waves in the distribution of pairwise genetic differences. *Mol. Biol. Evol.* **1992**, *9*, 552–569. [[PubMed](#)]
40. Aboim, M.A.; Menezes, G.M.; Schlitt, T.; Rogers, A.D. Genetic structure and history of populations of the deep-sea fish *Helicolenus dactylopterus* (Delaroche, 1809) inferred from mtDNA sequence analysis. *Mol. Ecol.* **2005**, *14*, 1343–1354. [[CrossRef](#)]
41. Shen, K.N.; Tzeng, W.N. Reproductive strategy and recruitment dynamics of amphidromous goby *Sicyopterus japonicus* as revealed by otolith microstructure. *J. Fish Biol.* **2008**, *73*, 2497–2512. [[CrossRef](#)]
42. Iida, M.; Watanabe, S.; Shinoda, A.; Tsukamoto, K. Recruitment of the amphidromous goby *Sicyopterus japonicus* to the estuary of the Ota River, Wakayama, Japan. *Environ. Biol. Fish.* **2008**, *83*, 331–341. [[CrossRef](#)]
43. Excoffier, L.; Lischer, H.E. Arlequin suite ver. 3.5: A new series of programs to perform population genetics analyses under Linux and Windows. *Mol. Ecol. Resour.* **2010**, *10*, 564–567. [[CrossRef](#)]
44. Excoffier, L.; Smouse, P.E.; Quattro, J.M. Analysis of molecular variance inferred from metric distances among DNA haplotypes: Application to human mitochondrial DNA restriction data. *Genetics* **1992**, *131*, 479–491. [[CrossRef](#)]
45. Stanley, H.F.; Casey, S.; Carnahan, J.M.; Goodman, S.; Harwood, J.; Wayne, K. Worldwide patterns of mitochondrial DNA differentiation in the harbor seal (*Phoca vitulina*). *Mol. Biol. Evol.* **1996**, *13*, 368–382. [[CrossRef](#)]
46. Tajima, F. Statistical method for testing the neutral mutation hypothesis by DNA polymorphism. *Genetics* **1989**, *123*, 585–595. [[CrossRef](#)] [[PubMed](#)]
47. Fu, Y.X. Statistical tests of neutrality of mutations against population growth, hitchhiking and background selection. *Genetics* **1997**, *147*, 915–925. [[CrossRef](#)] [[PubMed](#)]
48. Mantel, N. The detection of disease clustering and a generalized regression approach. *Cancer Res.* **1967**, *27*, 209–220.
49. Sezmis, E. The Population Genetic Structure of *Portunus pelagicus* in Australian Waters. Ph.D Thesis, Murdoch University, Perth, Australia, 2004.
50. Crandall, K.A.; Templeton, A.R. Empirical tests of some predictions from coalescent theory with applications to intraspecific phylogeny reconstruction. *Genetics* **1993**, *134*, 959–969. [[CrossRef](#)] [[PubMed](#)]
51. Chiang, T.Y.; Schaal, B.A. Phylogeography of North American populations of the moss species *Hylocomium splendens* based on the nucleotide sequence of internal transcribed spacer 2 of nuclear ribosomal DNA. *Mol. Ecol.* **1999**, *8*, 1037–1042. [[CrossRef](#)]
52. Wang, J.P.; Hsu, K.C.; Chiang, T.Y. Mitochondrial DNA phylogeography of *Acrossocheilus paradoxus* (Cyprinidae) in Taiwan. *Mol. Ecol.* **2000**, *9*, 1483–1494. [[CrossRef](#)]
53. Li, N.S.; Zhao, S.; Wasiliev, B. *Geology of Marginal Sea in the North West Pacific*; Heilongjiang Education Press: Harbin, China, 2000. (In Chinese)
54. Ren, G.; Ma, H.; Ma, C.; Wang, W.; Chen, W.; Ma, L. Genetic diversity and population structure of *Portunus sanguinolentus* (Herbst, 1783) revealed by mtDNA COI sequences. *Mitochondrial DNA Part A* **2017**, *28*, 740–746. [[CrossRef](#)]
55. Grant, W.S.; Bowen, B.W. Shallow population histories in deep evolutionary lineages of marinefishes: Insights from sardines and anchovies and lessons for conservation. *J. Hered.* **1998**, *89*, 415–426. [[CrossRef](#)]
56. Ma, H.Y.; Ma, C.Y.; Li, C.H.; Lu, J.X.; Zou, X.; Gong, Y.Y.; Wang, W.; Chen, W.; Ma, L.; Xia, L.J. First mitochondrial genome for the red crab (*Charybdis feriata*) with implication of phylogenomics and population genetics. *Sci. Rep.* **2015**, *5*, 11524. [[CrossRef](#)]
57. Xu, J.; Chu, K.H. Genome scan of the mitten crab *Eriocheir sensu stricto* in East Asia: Population differentiation, hybridization and adaptive speciation. *Mol. Phylogenet. Evol.* **2012**, *64*, 118–129. [[CrossRef](#)]
58. Abdul Halim, S.A.A.; Othman, A.S.; Akib, N.A.M.; Jamaludin, N.A.; Esa, Y.; Nor, S.A.M. Mitochondrial markers identify a genetic boundary of the Green Tiger Prawn (*Penaeus semisulcatus*) in the Indo-Pacific Ocean. *Zool. Stud.* **2021**, *60*, 8.
59. Benzie, J.A.H.; Williams, S.T. Genetic structure of giant clam (*Tridacna maxima*) populations in the West Pacific is not consistent with dispersal by present-day ocean currents. *Evolution* **1997**, *51*, 768–783.

60. Dall, W.; Hill, J.; Rothlisberg, P.C.; Staples, D.J. *The Biology of Penaeidae*. *Advances in Marine Biology* 27; Blaxter, J.H.S., Southward, A.J., Eds.; Academic Press: New York, NY, USA, 1990.
61. Wenner, A.M. Sex ratio as a function of size in marine Crustacea. *Am. Nat.* **1972**, *106*, 321–350. [[CrossRef](#)]
62. Campbell, G.R.; Fielder, D.R. Size at sexual maturity and occurrence of ovigerous females in three species of commercially exploited portunid crabs in S.E. Queensland. *Proc. R. Soc. Qld.* **1986**, *97*, 79–87.
63. Kepel, A.A.; Tsareva, L.A. First record of tropical crabs *Portunus sanguinolentus* (Herbst, 1783) and *Plagusia depressatuberculata* Lamarck, 1818 in Peter the Great Bay, Sea of Japan. *Russ. J. Mar. Biol.* **2005**, *31*, 124–125. [[CrossRef](#)]
64. Chan, B.K.K.; Tsang, L.M.; Chu, K.H. Morphological and genetic differentiation of the acorn barnacle *Tetraclita squamosa* (Crustacea, Cirripedia) in East Asia and description of a new species of Tetraclita. *Zool. Scr.* **2007**, *36*, 79–91. [[CrossRef](#)]
65. Tsang, L.M.; Wu, T.H.; Shih, H.T.; Williams, G.A.; Chu, K.H.B.; Chan, K.K. Genetic and morphological differentiation of the Indo-West Pacific intertidal barnacle *Chthamalus malayensis*. *Integr. Comp. Biol.* **2012**, *52*, 388–409. [[CrossRef](#)]
66. Wong, K.J.H.; Chan, B.K.K.; Shih, H.T. Taxonomy of the sand bubbler crabs *Scopimera globosa* De Haan, 1835, and *S. tuberculata* Stimpson, 1858 (Crustacea: Decapoda: Dotillidae) in East Asia with description of a new species from the Ryukyus, Japan. *Zootaxa* **2010**, *2345*, 43–59. [[CrossRef](#)]